Modeling of 3D microstructures produced by additive manufacturing

Cite as: AIP Conference Proceedings **2051**, 020256 (2018); https://doi.org/10.1063/1.5083499
Published Online: 12 December 2018

V. Romanova, O. Zinovieva, R. Balokhonov, A. Zinoviev, V. Ploshikhin, E. Emelianova, and M. Sergeev.

Modeling of 3D Microstructures Produced by Additive Manufacturing

V. Romanova[1,a)], O. Zinovieva[2,b)], R. Balokhonov[1,c)], A. Zinoviev[2,d)], V. Ploshikhin[2,e)], E. Emelianova[1,3,f)], and M. Sergeev[1,3,g)].

[1] *Institute of Strength Physics and Materials Science SB RAS, Tomsk, 634055 Russia*
[2] *Airbus endowed Chair for Integrative Simulation and Engineering of Materials and Processes, University of Bremen, Bremen, Germany*
[3] *National Research Tomsk State University, Tomsk, 634050 Russia*

[a)] Corresponding author: varvara@ispms.tsc.ru
[b)] zinovieva@isemp.de
[c)] rusy@ispms.tsc.ru
[d)] zinoviev@isemp.de
[e)] ploshikhin@isemp.de
[f)] emelianova@ispms.tsc.ru
[g)] sergeevmaximv@gmail.com

Abstract. Two approaches to simulating microstructures typical of additively manufactured (AM) materials are presented. First approach relies on the mathematical description of the microstructure evolution during metal AM process, taking into account complex physical processes involved. The numerical solution is based on a combination of the finite difference method for modeling AM thermal processes and the cellular automata method for describing the grain growth. The other approach provides fast generation of artificial 3D microstructures similar to those produced by AM by geometrical characteristics of grains, using the step-by-step packing method.

INTRODUCTION

Additive manufacturing (AM) is an innovative technology which enables producing structural components of complex geometry. Although considerable progress in this field has been attained in the past few years, many problems remain to be unsolved yet. Particularly, there is still a great deal to learn about the deformation and fracture mechanisms developing in AM materials since their microstructure and mechanical properties are much different from those of as-received materials [1, 2]. The micromechanical numerical analysis with explicit consideration of the material microstructure (see, e.g., [3–5]) seems to be a reasonable tool for analyzing the AM material behavior which is difficult to be predicted within macroscopic approach.

The first step in the numerical analysis implies the construction of a microstructural geometrical model which would be further used as input data in the boundary-value problem. Being a nontrivial task in a 2D case, this task becomes even much more complicated in three dimensions. In this paper, two approaches to simulating AM microstructures of an aluminum alloy are presented. First approach relies on the mathematical description of the microstructure evolution during AM process, taking into account complex physical processes involved. The numerical solution is based on a combination of the finite difference (FD) method for modeling AM thermal processes and the cellular automata (CA) method for describing the grain growth [6]. Another approach provides fast generation of artificial 3D microstructures similar to those produced by AM by the grain geometry, using the method of step-by-step packing (SSP) [5].

Proceedings of the Advanced Materials with Hierarchical Structure for New Technologies and Reliable Structures
AIP Conf. Proc. 2051, 020256-1–020256-5; https://doi.org/10.1063/1.5083499
Published by AIP Publishing. 978-0-7354-1777-9/$30.00

EXPERIMENTAL DATA

A strong morphological and crystallographic texture has been observed in some alloy systems produced by metal AM [1, 6–8]. As an example, an EBSD image of a front view of 316L steel produced by selective laser melting (SLM) is shown in Fig. 1a. Elongated columnar grains are reported to grow across multiple layers, reaching several millimeters in height. In metal AM, a part of the previously deposited layer or the baseplate in the case of the first layer is remelted. The dominant mechanism of solidification during metal AM is the epitaxial growth of partially melted grains from the previous layers. This results in coarse columnar structures nearly always observed in the AM metal specimens [1, 6–8].

The crystallographic texture is the result of the following three phenomena. First, nucleation of new grains in the melt is unlikely and negligible. Secondly, as a result, the epitaxial growth takes place, where a grain grows over a layer preserving the orientation. Consequently, the solidification structure consists of elongated columnar grains. Thirdly, a natural selection of grains with a small angle between their ⟨100⟩ direction and the thermal gradient take place during solidification [10]. Unfavorably oriented grains are eliminated in the build direction, and the distribution of grain orientations becomes biased toward certain angles. The direction of grain growth, defining the crystallographic texture of the AM material, may closely align with the build direction or deviate from it [1, 7, 8]. The crystallographic texture in the final AM material is assumed to be strongly affected by the melt pool shape and size [8].

MODELING OF GRAIN STRUCTURE EVOLUTION UNDER AM CONDITIONS

The cellular automata-finite difference (CAFD) approach to simulate the grain structure evolution during powder-bed based AM can be divided into two main stages, namely, preprocess and process. In the preprocess stage, we input data necessary for the simulation such as material properties, process parameters, initial and boundary conditions, and generate the baseplate microstructure (Fig. 1b). In the process stage, we calculate the transient heat transfer, obtain a new field of phases (or CA states) and simulate the grain structure evolution. The cycle of steps in the process stage is repeated until the whole computational domain is considered as solidified. Brief particularities of the CAFD model will be described. Please refer to [6] for further details on the CAFD model.

The Goldak double ellipsoid model is adopted to describe heat input from a moving heat source [10]. In geometric sense, the model combines two semi-ellipsoids. The heat is distributed in a Gaussian manner over these semi-ellipsoid areas.

Growth rate of grains is defined as a function of local undercooling. Its calculation is based on the Kurz–Giovanola–Trivedi model [11]. In order to speed up the calculations, a relationship between growth rate and undercooling is fitted with a polynomial approximation.

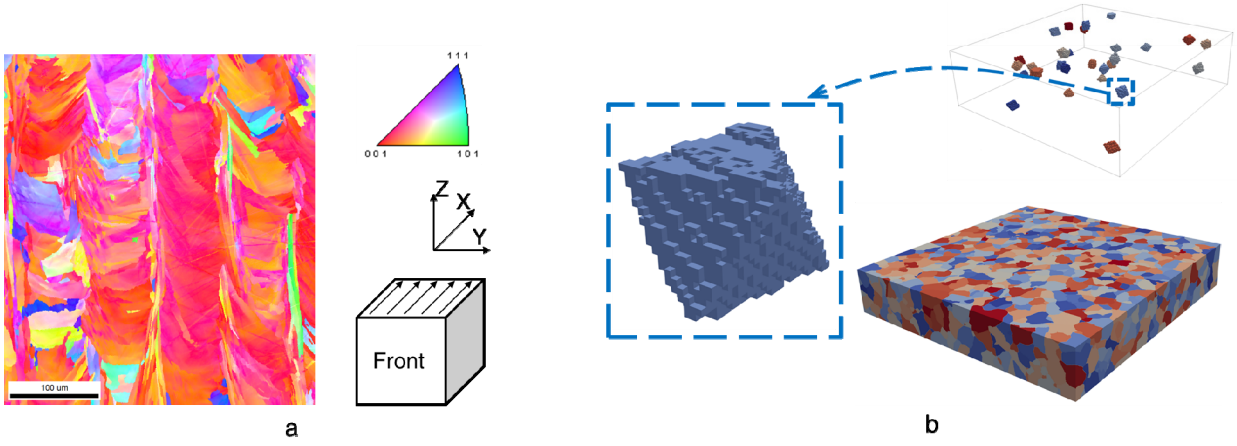

FIGURE 1. (a) EBSD image of the front view (*YZ*-plane) of SLM 316L steel. The EBSD inverse pole figure image is represented with the crystal orientations along the build direction *Z*; (b) CAFD generation of the polycrystalline baseplate

We are interested in mesoscale simulations, i.e. we do not take into account a complex morphology of the solidification grain and consider a concept of a grain envelope, which separates the inner space of the grain, including a solid dendrite and interdendritic liquid, from the exterior. Since materials with a cubic lattice are considered, the envelope can be described by an octahedron (Fig. 1b). Vectors lying on the diagonals of the octahedron correspond to the ⟨100⟩ crystallographic directions. Along these directions main dendrite arms grow.

CA approach for grain growth modeling is known to suffer from artificial anisotropy caused by the mesh. To solve this problem, a modified decentred octahedron growth technique is adopted [11].

Let us dwell briefly on the main steps that enable simulations of the grain structure evolution during the powder-bed-based AM. In this work, we consider selective laser melting. The process begins with the simulation of a non-textured polycrystalline baseplate with equiaxed grains. The multiple grain nucleation and growth in the uniform temperature field is simulated. For the simulation of non-textured material, we use an original approach described in detail in [6]. The generated baseplate data together with the material properties, heat source parameters and a CLI-file defining the scanning strategy for each layer build up an input for the process simulation. A powder layer is then generated upon the solidified material. The heat source starts moving according to the predefined strategy. Heat source locally heat and melts the material, which subsequently solidifies. As soon as all the cells become solid, a new powder layer is generated. The procedure is repeated until a specified number of layers are simulated.

Figure 2 shows the final grain structure produced in the SLM simulation. Colors represent misorientation angles between *Z*-axes of specimen (global) and crystal (local) coordinate systems. We consider unidirectional scanning strategy, without rotation of the scanning direction (*X* = along-scan). The computational domain is discretized by a regular $500 \times 500 \times 1418$ mesh with hexahedral elements. The polycrystalline baseplate consists of 8594 equiaxed grains. The SLM specimen consists of large columnar grains, which originate from the baseplate and the powder surrounding the specimen and grow epitaxially.

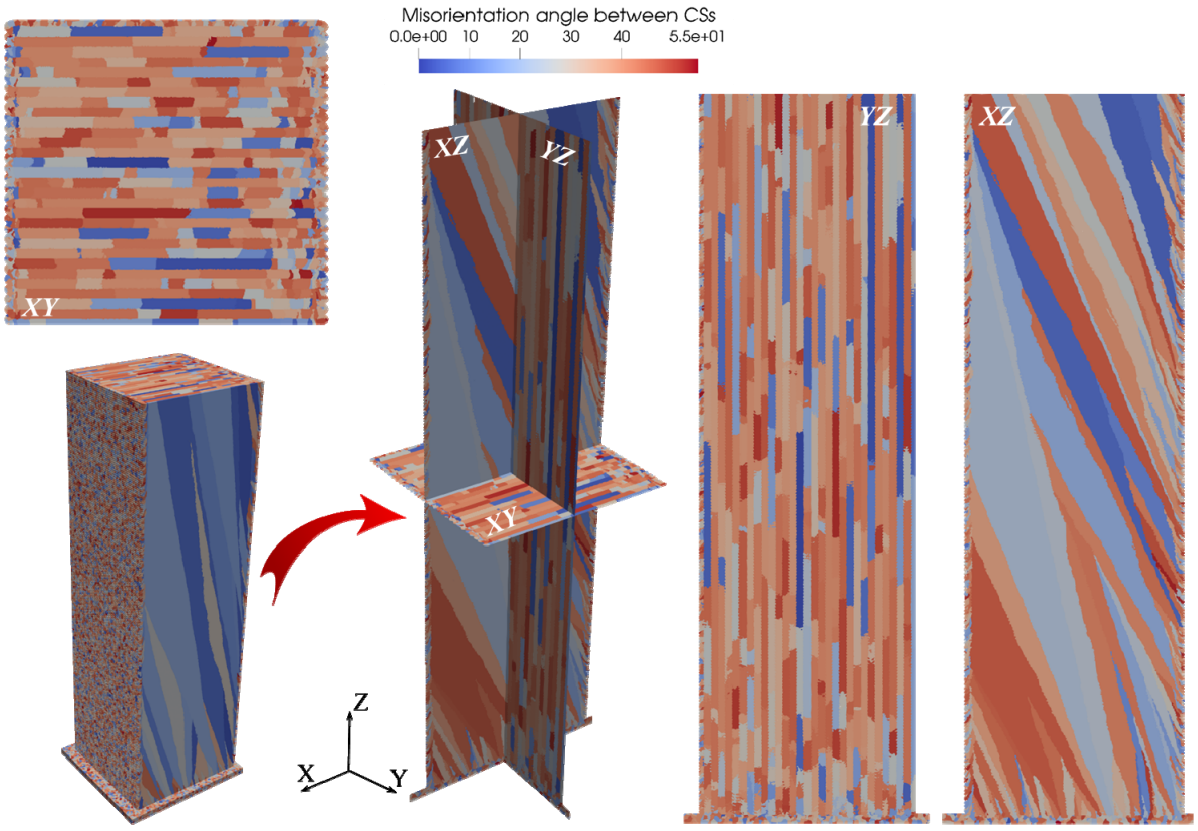

FIGURE 2. Final grain structure obtained in the SLM simulation and grain structures in the middle cross-sections of the model SLM specimen. Laser beam moved along the *X*-axis. Cross-sections are labeled in the same places as in the 3D view to show their relative location

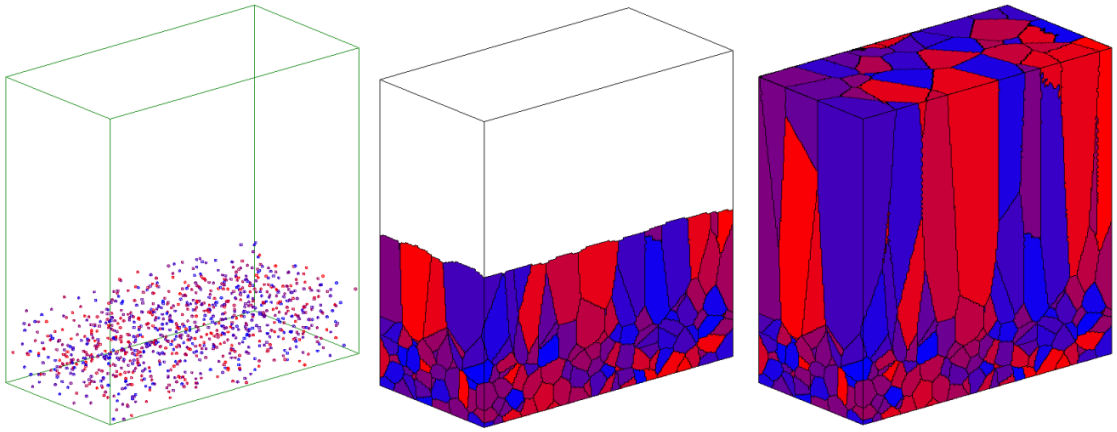

(a) (b) (c)

FIGURE 3. SSP-design of an AM-produced microstructure: (a) seed distribution; (b) an intermedium step; (c) resulting structure

In the *YZ*-plane, columnar grains appear along the build direction, with the boundaries mostly being parallel to each other and the build direction. In the *XZ*-plane elongated grains show a strong tendency to follow the direction of the heat source movement and to tilt from the build direction. This agrees with experimental evidence (see Fig. 1a, [1, 6–8]).

SSP-DESIGN OF AN ARTIFICIAL AM MICROSTRUCTURE

To design a 3D model of an AM microstructure, the SSP method based on a combination of analytical and simulation tools has been used [5]. In the first step of the SSP design, the computational domain is discretized by a mesh, with coordinates being defined for each nodal point. Since the design of a microstructure precedes the task of simulating its mechanical behavior, the specimen geometry is defined from the conditions of an appropriate mechanical problem and the discretization parameters are dictated by the numerical method to be further applied. In a general case, an arbitrarily-shaped specimen can be discretized by a regular or irregular computational mesh and then packed with microstructural elements.

As the SSP input data, some mesh elements are selected to be seeds of microstructure constituents, with each kind of seeds being associated with a certain analytical law of growth. The seed distribution and growth law, the main parameters controlling microstructure geometry, can be chosen from the experimental data of, e.g., EBSD and X-ray analyses, optical microscopy, etc.

As the step-by-step packing procedure begins, the volumes surrounding the seeds are incremented by preset values in accordance with preset analytical laws of growth. For each mesh element belonging to none of the microstructural constituents it is checked whether coordinates of its central point fall within any of the growing volumes. If so, the mesh element is considered to belong to this microstructure component and excluded from further analysis. Such a procedure is repeated until the volume fraction of the growing microstructure has reached a preset value.

The SSP design of an AM-produced microstructure is illustrated in Fig. 3. The computational domain is discretized by a regular $200 \times 200 \times 100$ mesh with hexahedral elements. As input data, 1000 seeds are randomly distributed over the bottom part of the specimen as shown in Fig. 3a. All the grains are grown by the spherical law at the same growth velocity until the grain structure fills 100% specimen volume. The resulting polycrystal is characterized by equiaxed grains in the bottom part which is treated as a substrate and by elongated grains in the upper part similar to those observed in the experimental AM microstructures (see Fig. 1a, [1, 6–8]).

CONCLUSIONS

Two methods for construction microstructural models of AM materials have been presented. The models can be further used in the microscale stress-strain analysis of the AM-produced materials under loading. To do so, the grains should be associated with the crystal plasticity-based constitutive models taking into account the

microstructure and texture effects. In the subsequent analysis, the models will be implemented in the finite element and finite difference calculations.

ACKNOWLEDGMENTS

This work is supported by the Deutsche Forschungsgemeinschaft (Grant No. PL 584/4-1) and the Russian Foundation for Basic Research (Grant No. 18-501-12020). We also acknowledge Neue Materialien Bayreuth GmbH for providing us with the experimental data.

REFERENCES

1. M. Brandt, *Laser Additive Manufacturing: Materials, Design, Technologies, and Applications* (Woodhead Publishing, Sawston, 2017).
2. D. A. Ramirez, L. E. Murr, E. Martinez, et al., Acta Mater. **59**(10), 4088–4099 (2011).
3. Ig. S. Konovalenko, A. I. Dmitriev, A. Yu. Smolin, and S. G. Psakhie, Phys. Mesomech. **15**(1–2), 88–93 (2012).
4. V. A. Romanova, E. Soppa, S. Schmauder, and R. R. Balokhonov, Comput. Mech. **36**, 475–483 (2005).
5. V. Romanova, R. Balokhonov, and O. Zinovieva, Meccanica **51**, 359–370 (2016).
6. O. Zinovieva, A. Zinoviev, and V. Ploshikhin, Comput. Mater. Sci. **141**, 207–220 (2018).
7. L. Thijs, "Microstructure and texture of metal parts produced by selective laser melting", Ph.D. thesis, KU Leuven, 2014.
8. T. DebRoy, H. L. Wei, T. S. Zuback, et al., Prog. Mater. Sci. **92**, 112–224 (2017).
9. J. A. Dantzig and M. Rappaz, *Solidification* (EPFL Press, Switzerland, 2016).
10. J. Goldak, A. Chakravarti, and M. Bibby, Metall. Trans. B **15**(2), 299–305 (1984).
11. W. Kurz, B. Giovanola, and R. Trivedi, Acta Metall. **34**(5) 823–830 (1986).
12. W. Wang, P. D. Lee, and M. McLean. Acta Mater. **51**(10), 2971–2987 (2003).